

Macromolecular Materials and Engineering

Crosslinked PLA

Bone Tissue Engineering

Porous Scaffold

Tissue Repair

Biocompatible

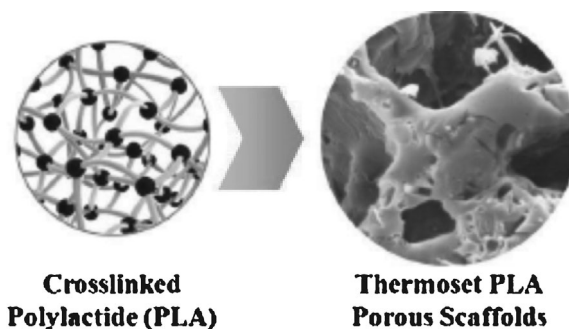
Biodegradable

1/2013

Fabrication of Polylactide-Based Biodegradable Thermoset Scaffolds for Tissue Engineering Applications

Reika Sakai, Baiju John, Masami Okamoto,* Jukka V. Seppälä, Jayasheelan Vaithilingam, Husnah Hussein, Ruth Goodridge

The fabrication of tissue engineering scaffolds based on the polymerization of crosslinked polylactide using leaching and batch foaming to generate well-controlled and interconnected biodegradable polymer scaffolds is reported. The scaffold fabrication parameters are studied in relation to the interpore connectivity, pore morphology, and structural stability of the cross-linked PLA scaffold. In vitro cell culture and in vitro degradation are used to analyze the biocompatibility and biodegradability of the scaffolds. The new crosslinked PLA thermoset scaffolds are highly suitable for bone tissue engineering applications due to their complex internal architecture, thermal stability, and biocompatibility.



1. Introduction

The regeneration of lost tissues or organs due accidents or disease is a major concern in modern health care. With tissue engineering, we can create biological substitutes to repair or replace the failing organs or tissues. One of the most promising approaches toward this direction is to grow cells on scaffolds-highly engineered structures that act as

temporary support for cells which facilitate the regeneration of the target tissues without losing the 3-D stable structure.^[1,2]

Polymeric scaffolds play a pivotal role in tissue engineering through cell seeding, proliferation, and new tissue formation in three dimensions. These scaffolds have shown great promise in the research of engineering a variety of tissues. Pore size, porosity, and surface area are widely recognized as important parameters for a tissue engineering scaffold. Other architectural features such as pore shape, pore wall morphology, and interconnectivity between pores of the scaffolding materials are also suggested to be important for cell seeding, migration, growth, mass transport, and tissue formation.

The natural scaffolds made from collagen are fast replaced with ultraporous scaffolds from biodegradable polymers. Biodegradable polymers have been attractive candidates for scaffolding materials because they degrade as the new tissues are formed eventually leaving nothing foreign to the body. The major challenges in the scaffold manufacture lies in the design and fabrication of

R. Sakai, B. John, M. Okamoto

Advanced Polymeric Nanostructured Materials Engineering,
Graduate School of Engineering, Toyota Technological Institute,
2-12-1 Hisakata, Tempaku, Nagoya, 468 8511, Japan

E-mail: okamoto@toyota-ti.ac.jp

J. V. Seppälä

Department of Biotechnology and Chemical Technology, School
of Chemical Technology, Aalto University, P.O. Box 16100
FI-00076, Aalto, Finland

J. Vaithilingam, H. Hussein, R. Goodridge

The Wolfson School of Mechanical and Manufacturing
Engineering, Loughborough University, Leicestershire, LE11 3TU,
UK

customizable biodegradable constructs with desirable properties that promote cell adhesion and cell porosity along with sufficient mechanical properties that match the host tissue with predictable degradation rate and biocompatibility.^[3,4]

Thermoplastic polylactide (PLA) nanocomposite foams and scaffolds are becoming popular these days with its biodegradable and biocompatible nature.^[5–9] However, the research on PLA-based thermoset scaffolds are at its infancy, which may find more suitable with predictable degradability, thermal stability, and mechanically viable as compared with the thermoplastic ones.

In this research, we conducted the fabrication of highly porous and interconnected biodegradable polymer scaffolds based on the polymerization of crosslinked PLA produced using a salt particulate leaching method and the one prepared by a combination of batch foaming followed by leaching. The scaffold fabrication procedure involved two simple steps, radical crosslinking polymerization of PLA oligomers and subsequent salt leaching or foaming and leaching. This method renders the scaffold fabrication facile, rapid, and easily achievable. The microarchitectural properties of the crosslinked PLA scaffold, in particular its morphology, porosity distribution, and structural stability, were analyzed and correlated with the results of the *in vitro* cell culture analyzed with the cell/scaffold interaction using the colonization of human mesenchymal stem cells (hMSCs) and degradation using phosphate-buffered saline (PBS) solution.

2. Experimental Section

2.1. Preparation of Crosslinked PLA Resin

The initial step is the synthesis of branched PLA oligomers from PLA using ring opening reaction with linear/branched polyols. The PLA oligomers was synthesized from the polymerization of D,L-lactide in a batch reactor at 160 °C for 3 h with 0.02 mol% Sn(II) octoate as an initiator with an appropriate amount of coinitiators.

The telechelic D,L-lactide-based oligomers so prepared was functionalized with methacrylic anhydride for 3 h at 120 °C, and the final product was purified by distillation under reduced a pressure at 140 °C. The resultant PLA oligomer was designated as Lait-X. For crosslinking, 2,5-bis(*tert*-butylperoxy)-2,5-dimethylhexane (1 wt%, Sigma-Aldrich Co.) is mixed with Lait-X and cured at 150 °C for 10 h.

2.2. Fabrication of PLA Thermoset Scaffolds

The NaCl crystals (Salt Industry Center, Japan) were powdered to a particle size from 450 to 30 μm by grinding in a ceramic mortar with subsequent drying in a ceramic hot plate (CHP-170D, AS ONE Co.) at 120 °C for 1 h. The size of the NaCl particles was calculated from the polarized optical images and averaged using an image analyzing software. Variation of size in the NaCl particles was preferable for generating pores with good interconnectivity between the pores. Sample suspensions prepared for the scaffold fabrication consists of the PLA oligomer resin (Lait-X), radical initiator, and NaCl particles. The Lait-X/initiator/salt mixture was stirred with a spatula for a few minutes until the mixture had completely wet the NaCl crystals. For all the samples the crosslinked PLA was mixed with NaCl at around 60 °C except the Lait-X/e sample (Table 1). The Lait-X/e treated with acetone to reduce the viscosity was dried in a vacuum drying oven (DP33, YAMATO SCIENTIFIC Co., Ltd.) at room temperature. The composite mixture was added into a Teflon mold (a cubical vial of dimension: 2 × 2 × 2 cm³). A rigorous curing process was applied to all samples in a hot air oven (ST-110, ESPEC Co.) at 150 °C for 10 h. One of the cured samples with the salt particulate (Lait-X/c) was taken for foaming using batch process under supercritical carbon dioxide (20 MPa) for 5 h at 80 °C in an autoclave (TSC-WC-0096, Taiatsu Techno Co.).^[9] The prepared disks were soaked in a large volume of deionized ultrapure water (specific resistance 18 MΩ · cm, TOC < 20 ppb, WR600A, YAMATO SCIENCE Co., Ltd.) for 48 h to leach the salt particulate leaving the porous scaffold. The water was refreshed twice every day to favor the complete dissolution of the salt. The fabricated scaffold samples were collected, dried, and stored in a desiccator. The dimension of the prepared scaffold was 1 × 1 × 0.2 cm³.

Table 1. Properties of crosslinked PLA scaffolds.

Sample	Composition ratio (Lait-X/NaCl/acetone) [wt%]	Particle size [μm]	Specific gravity	T _g [°C]
Lait-X/a	1/1/0	450	0.69	39.9
Lait-X/b	1/1.2/0	30	0.74	37.6
Lait-X/c ^{a)}	1/1.2/0	30	–	37.4
Lait-X/d	1/1/0	30	0.82	41.6
Lait-X/e	1/4/0.4	450	0.57	40.7
Lait-X	1/0/0	–	1.42	34.5

^{a)}The scaffold is prepared through batch foaming followed by leaching.

2.3. In vitro Cell Culture

Human mesenchymal stem cells (hMSCs) were used for in vitro cell culture to analyze the biocompatibility. This was prepared by mixing 10^6 hMSCs into 50 mL of mesenchymal stem cell basal medium (MSCBM) in a flask and incubated for 3 d. A 10 mL of PBS (pH = 7.4) was added to the medium and drained, to which a 10 mL of trypsin was added and kept for incubation. This medium was put into a centrifuge at 5 g for 5 min to sediment the hMSCs cells. The removed hMSCs was standardized to 1200 μ L with MSCBM. Meanwhile scaffold samples along with cell culture plates were sterilized with ethanol at room temperature and subsequent irradiation with UV for 24 h. A 300 μ L of the MSCBM medium composed of hMSCs was added to each cell culture plate with the scaffold and placed in an incubator (37 °C, 5% CO₂). The cell culture media was changed every 2nd and 5th with the cell activity checked on the 6th day. The cell number and concentration was analyzed through hemocytometer with histological staining using trypan blue. The cell activity was analyzed through a plate reader (BIO TEK, ELx800) stained with alamar blue in the wavelength range of 570–600 nm. The coloration was estimated through absorbance values. A control was set with scaffold in MSCBM medium without the hMSCs.

2.4. In vitro Degradation

PBS (pH = 7.4) that simulated the ionic concentrations of the human body was used to assess the biodegradability. PBS was prepared by mixing two solutions; 18.2 vol% of 1/15 M KH₂PO₄ (9.078 g KH₂PO₄ per liter of H₂O) and 81.8 vol% of 1/15 M Na₂HPO₄ (11.876 g Na₂HPO₄ · 2H₂O per liter of H₂O), was based on ISO 15814: 1999(E). A 100 mL PBS was added to an inert plastic container with the scaffold samples and sealed with paraffin. All containers were kept in an incubator at 37.5 ± 0.5 °C. The pH values were checked frequently and adjusted to 7.4 ± 0.3 using 0.1 M of NaOH. In order to estimate the weight losses, the scaffold was taken out and air dried at 33 °C for 24 h with the duration of 2 and 4 weeks.

2.5. Characterization

NaCl crystal particles were observed using a polarization optical microscope (POM, OPTIPHOTO2-POL, Nikon Co.). The size of the particles was determined by analyzing the POM images with Image J 1.43u software (National Institutes of Health, US).

The morphological features of the Lait-X Scaffolds were analyzed with a scanning electron microscope (SEM, JSM-5310LV JEOL Ltd.) coated with gold and palladium (Au/Pd 60:40). The specific gravity measurements were conducted to analyze the completion of salt leaching by MD-200S, Alfa Mirage Co., Ltd. All samples were tested over five times and average values were calculated. The morphological features of the scaffold undergone in vitro degradation was observed by field-emission scanning electron microscopy [FE-SEM, Carl Zeiss (Leo) 1530 VP], operated at 5 kV with a coating of gold and palladium.

Pore size distribution was measured by mercury porosimetry (Shimadzu Techno-Research, AutoPore IV9500 supplied by Micromeritics). From this measurement, porosity, total intrusion volume, total pore area, the average pore diameters were calculated.

Washburn's equation^[10] was used to calculate the pore size distribution through mercury porosimetry as

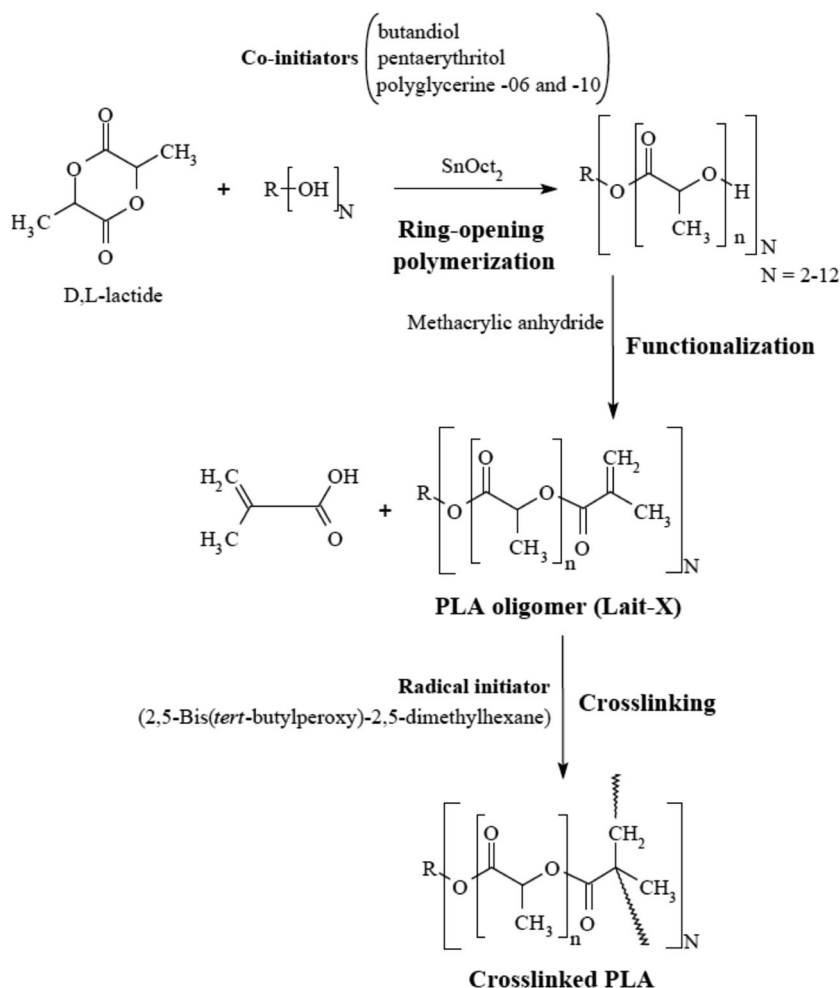
$$\pi r^2 p = -2\pi r \gamma \cos \theta \quad (1)$$

This equation assumes that the mercury intrude a cylindrical pore. The terms r , γ , θ , p represent the radius of the cylindrical pore, surface tension, contact angle, and pressure of mercury, respectively. The contact angle ($\theta = 130^\circ$) and the surface tension ($\gamma = 485 \times 10^{-5} \text{ mN} \cdot \text{m}^{-1}$) are constants while the radius of the cylinder (r) and pore size distribution are measured from the applied pressure (p) for the mercury intrusion.

The thermal properties were analyzed using the differential scanning calorimetry (DSC 2920, TA Instruments) at a heating rate of 5 °C · min⁻¹ from -50 to 250 °C in a powder form with a sample weight of 10 mg.

3. Results and Discussion

The preparation scheme of PLA oligomers resin (Lait-X) is shown in Figure 1.^[11–13] The initial step is the synthesis of branched PLA oligomers from PLA using ring opening reaction with linear/branched polyols. The PLA oligomer so prepared is functionalized and the final product was purified by distillation under a reduced pressure. The crosslinked PLA thermoset scaffolds were prepared by curing the Lait-X resin using initiator with NaCl as the particulate added to it. The salt particulate was leached through water leaving the porous scaffold. In the salt leaching method, the salt particles are influenced by gravity which results in the heterogeneous dispersion of the same leading to highly porous scaffold. One set of the cured Lait-X resin with particulate was foamed using batch process with subsequent leaching through water leading to a scaffold. The crosslinked PLA scaffold specimens were named as Lait-X/a-e based on the composition ratio of NaCl, PLA oligomer resin, and acetone used for the scaffold fabrication (Table 1). Acetone was used as a solvent to reduce the viscosity of the resin in Lait-X/e sample. Lait-X/b and Lait-X/c possess the same composition with the former prepared by salt leaching and the latter by batch foaming followed by leaching. For comparison, the suspension composed of neat Lait-X was also polymerized. The NaCl particle size for Lait-X/a, Lait-X/b, Lait-X/c, Lait-X/d, and Lait-X/e were 450, 30, 30, 30, and 450 μ m. The crosslinked PLA resin to NaCl ratios for Lait-X/a, Lait-X/b, Lait-X/c Lait-X/d, and Lait-X/e are 1:1, 1:1.2, 1:1.2, 1:1, and 1:4, respectively, with Lait-X/e having an additional ratio of 0.4 with the solvent acetone. The specific gravity of the scaffolds of Lait-X/a-e is reported in Table 1. The value of the specific gravity of scaffolds was much lower than the neat cured Lait-X sample (1.42) with Lait-X/e showing the lowest value. This is due to the volume increase from the pores after leaching and proves the



■ Figure 1. Scheme of synthesis of crosslinked PLA.

effectiveness of NaCl as the selective particulate for the scaffold fabrication.

Figure 2 presents the magnified views on the internal morphology of the crosslinked PLA scaffolds. Lait-X/a has no pore connectivity and has thicker walls between the consecutive pores (Figure 2a) in the size range of 450 μm . The Lait-X/b and Lait-X/c have the same percent of salt particulate with similar particle size; the former was turned into scaffold through simple leaching while the latter was through batch foaming followed by leaching (Table 1). The qualitative evaluation of the SEM images of Lait-X/b and Lait-X/c showed a well-developed porosity and interconnectivity with pore sizes spanning over a very wide range, from few μms to hundreds of μms (Figure 2b and c). Even though the Lait-X/d sample had a similar particulate particle size as Lait-X/b and Lait-X/c with good porosity the interconnectivity was very low (Figure 2d). The interconnectivity of pores is a significant parameter for porous scaffolds which plays a significant role in tissue develop-

ment through cell seeding, adsorption of H_2O , nourishments, and desorption of wastes. In Lait-X/e, acetone was used as a solvent, had a negative effect on the final outcome of the scaffold as shown in Figure 2e. The internal morphology of Lait-X/e after polymerization shows that pore walls are brittle and often broken with poor pore connectivity. The brittle nature of scaffolds shall affect the flexibility needed to substitute with the bone tissues. The scaffolds prepared with the smaller salt crystal sizes are robust with greater porosity (Lait-X/b and Lait-X/c). This is attributed to the agglomeration of the smaller crystals with short polymer domains during the curing process. When the cured salt/resin composite was soaked in water, the salt crystals are washed out leaving well connected pores with intricate internal architecture.

Figure 3 shows the relation between the pore size diameter to the cumulative and differential intrusions of mercury in Lait-X/b and Lait-X/c scaffolds. The maximum intrusion and interconnectivities of Lait-X/b was from 0.1 to 1 μm pore diameter regions and for Lait-X/c it was from 0.1 to 10 μm . The porosity, total intrusion volume, total pore area, and median pore diameter (volume) of Lait-X/b calculated by mercury porosimetry were 43%, 0.511 $\text{mL} \cdot \text{g}^{-1}$, 13.4 $\text{m}^2 \cdot \text{g}^{-1}$, and 0.520 μm whereas for Lait-X/c it was 49%, 0.688 $\text{mL} \cdot \text{g}^{-1}$,

27.6 $\text{m}^2 \cdot \text{g}^{-1}$, and 1.26 μm , respectively. The shift in the values of Lait-X/b and Lait-X/c was due to the effect of batch foaming which lead to the movement of salt particulate during foaming resulting in the increased porosity and total intrusion volume. The value of porosity that is best suited for the bone tissue scaffold lies in the range of 50%^[14,15] which matches with the porosity values of Lait-X/b and Lait-X/c.

The thermal behavior of the samples was analyzed using DSC thermograms (Table 1). There were no melting points (T_m), which demonstrates that all samples are amorphous and thermoset. The glass transition temperature (T_g) of neat Lait-X was 34.5 $^\circ\text{C}$ and for the scaffold sampled it varied between 39 and 41 $^\circ\text{C}$ with no significant variation. It also clear that there is no structural change in the scaffolds prepared with the simple particulate leaching and foaming followed by leaching. A significant difference in T_g is observed between the neat Lait-X and the scaffolds, which can be attributed to the hardening effect with the presence of NaCl particles while curing. The Lait-X thermoset scaffolds

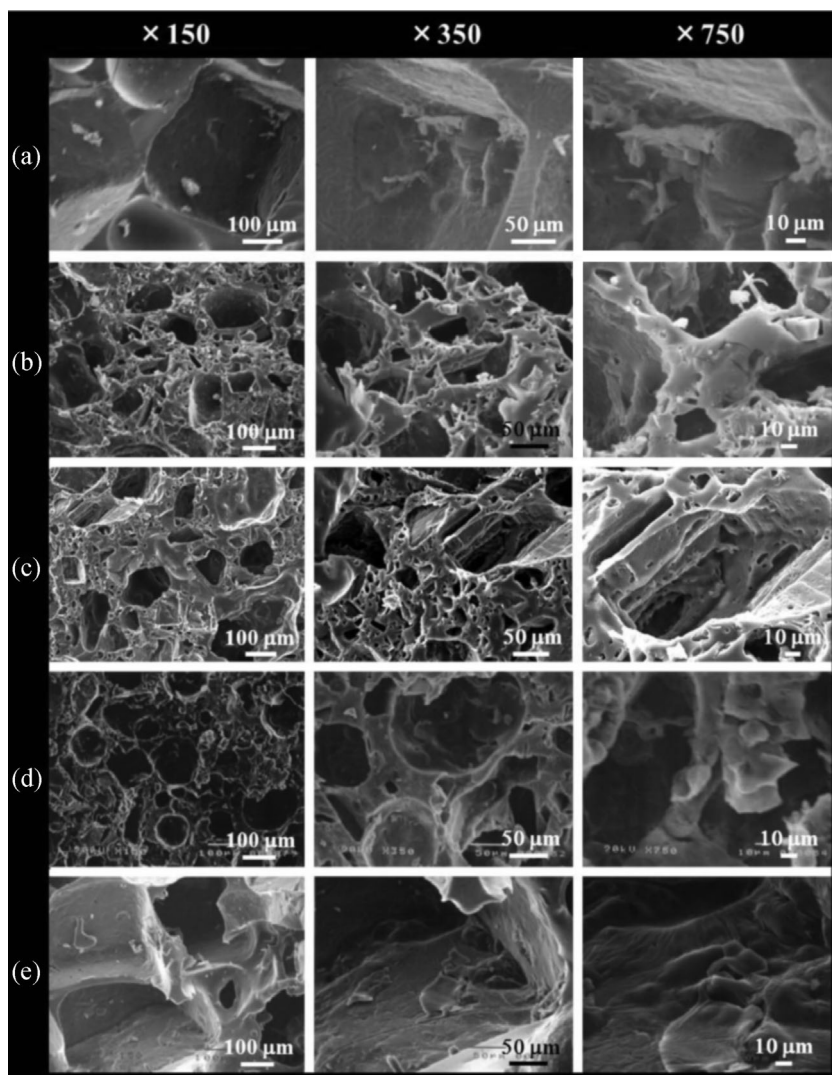


Figure 2. SEM images of crosslinked PLA porous scaffolds (a) Lait-X/a, (b) Lait-X/b, (c) Lait-X/c, (d) Lait-X/d, and (e) Lait-X/e for 150 \times , 350 \times , and 750 \times magnifications.

are thermally stable, possess a T_g that matches with the human body temperature, is an added advantage towards the potential application as a tissue engineering scaffold.

Figure 4 depicts the cell activities of Lait-X/b and Lait-X/c scaffolds in the culture plates analyzed with alamar blue assay using a plate reader. The control with scaffold in MSCBM medium without the hMSCs had a violet color while the ones with cell activities had a pink coloration. The number of cells in the cell culture plate with the scaffold sample was roughly 7.75×10^5 cells \cdot sample $^{-1}$ as enumerated from hemocytometer using trypan blue. Lait-X/b showed more cellular activity (Figure 4a and b) than the Lait-X/c with a variation the pink coloration even though both have same composition and varies only in the preparation method. This may be due to the effect of pore

wall regions in Lait-X/b that can promote the cellular adhesion and growth. Figure 4c shows the absorbencies of Lait-X/b and Lait-X/c with the cellular activity assessed using alamar blue. It confirms that Lait-X/b scaffolds have a high level of cell activity and superior biocompatibility which promoted the hMSCs adhesion leading to the increased cell activity. This result conforms to the observation of in vitro biodegradation discussed in the later section. The Lait-X/b and Lait-X/c were nontoxic and the cells seeded into the scaffolds exhibited the ability to attach and propagate in the scaffold structure.

The biodegradability of porous Lait-X/b and Lait-X/c thermoset scaffold were investigated in PBS solution at 37.5 °C by analyzing the loss of weight and pore morphology throughout degradation. The Lait-X/b and Lait-X/c were degraded almost completely within 4 weeks (Figure 5a and b). Both the scaffolds showed significant degradation after 2 weeks of immersion in PBS and total disintegration in another 2 weeks. The weight after in vitro degradation was nearly 49.4% for Lait-X/b and 58.8% for Lait-X/c due to the loss of the material into the PBS media with 2 weeks of exposure (Figure 5c). The increased disintegration of Lait-X/c over Lait-X/b was due to the increased surface area and porosity attained through foaming. The disintegration of the crosslinked PLA occurred to the monomer level and later to elemental level as confirmed from Figure 5a and b. Thus there are no harmful or nondisintegrative byproducts that harm or remain in

the biological system with its use. Although the porous scaffold was made from crosslinked PLA, the hydro-sensitive ester bonds facilitated the absorption and diffusion of water initiating the degradation. This rate of biodegradation is best suited for bone tissue regenerating application in children where the ones with faster regeneration are preferred. The T_g of PLA thermoset scaffold matched with the in vitro set temperature (37.5 °C) which influenced the degradation. This is an added advantage as it gives relevant flexibility when used for tissue repairs and regeneration. Figure 5d and e shows the morphological features of Lait-X/b and Lait-X/c under biodegradation in PBS solution through FE-SEM images after 2 weeks of degradation. The scaffolds retained the morphology with 50% weight loss after 2 weeks of degradation with

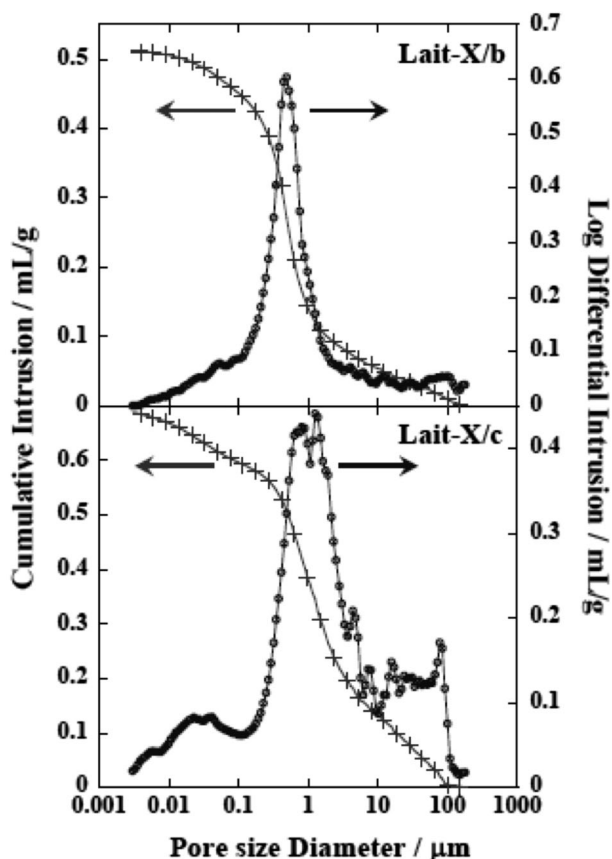


Figure 3. Pore size distribution in Lait-X/b and Lait-X/c scaffolds.

differences in features between the same. The spherical blisters were observed on the scaffold pore walls of Lait-X/b the scaffold samples due to degradation with the PBS (Figure 5d) and were not much visible with Lait-X/c. The spherical geometry was due to the impact of surface tension at the degradation points. The scaffolds possess a hetero-

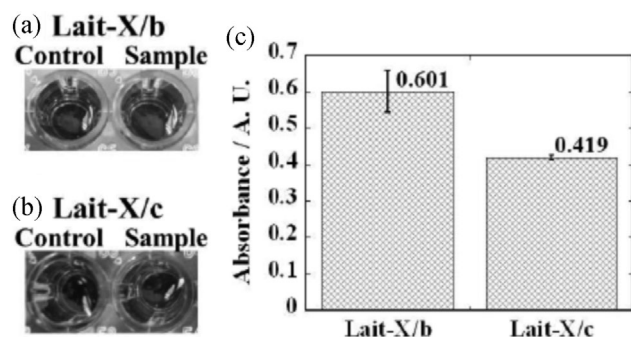


Figure 4. (a), (b) In vitro cell culture analysis of Lait-X/b and Lait-X/c showing the cell culture plates treated with alamar blue and (c) absorbance of Lait-X/b and Lait-X/c on the plate reader measured at a wavelength of 570–600 nm.

geneous morphology with numerous degradation points on scaffold pore wall regions which led to the fast degradation.

In fact it has been underlined that high porosity and biocompatibility shall boost osteogenesis in vivo, since bone regeneration involves vascularization, as well as recruitment and penetration of cells from the surrounding tissue.^[16] Moreover, 30–100 μm is usually considered the minimum required pore size to allow cell migration; vascularization and transportation processes.^[15] The Lait-X/b scaffold sample with excellent properties of thermally stability, biodegradability, and biocompatibility makes it a suitable candidate for bone tissue engineering scaffold. Moreover the well-developed network of interconnected pores which exceeds hundred μm shall boost osteogenesis. Unlike the scaffolds prepared by other techniques (e.g., freeze-drying, solvent casting, or liquid-liquid phase separation) the current process does not require any harmful solvents, thus reducing the potential of toxic reagents to leach out over time.

In the present scenario, bioceramics entities such as tricalcium phosphate, hydroxyapatite (HA), and bioactive glass have been used for bone tissue engineering scaffolds and drug delivery.^[17–21] Osteomyelitis is a most common medical problem related to bones caused by an inflammatory process leading to bone destruction caused by infective microorganisms found worldwide in children, where the bone tissue regeneration is required.^[22] Although, bioceramics scaffolds serve the purpose of tissue regeneration and drug release but they present formidable limitations such as the lack of information relating to the long-term effects in the body. The bioceramics especially HA when resorbed into the biological system for a long-term shall give secondary fixation (70% remains in dogs after 4 months and for humans it is 90% even after 4 years).^[23] HA crystals released from the bone scaffolds will accumulate in the joints and can stimulate an inflammatory response in the prosthesis area.^[24] In the case of children with acute osteomyelitis the PLA based thermoset scaffold can serve the purpose as it possess excellent biodegradability and biocompatibility with no side effects of byproducts or end products.

4. Conclusion

This work represented the first time that highly porous crosslinked PLA scaffolds were successfully prepared through particulate leaching and foaming followed by leaching methods. The scaffolds were porous with good interconnectivity and thermal stability. The SEM images confirmed the pore connectivity and structural stability of the crosslinked PLA scaffold. The in vitro cell culture demonstrated the ability of the scaffold to support hMSC

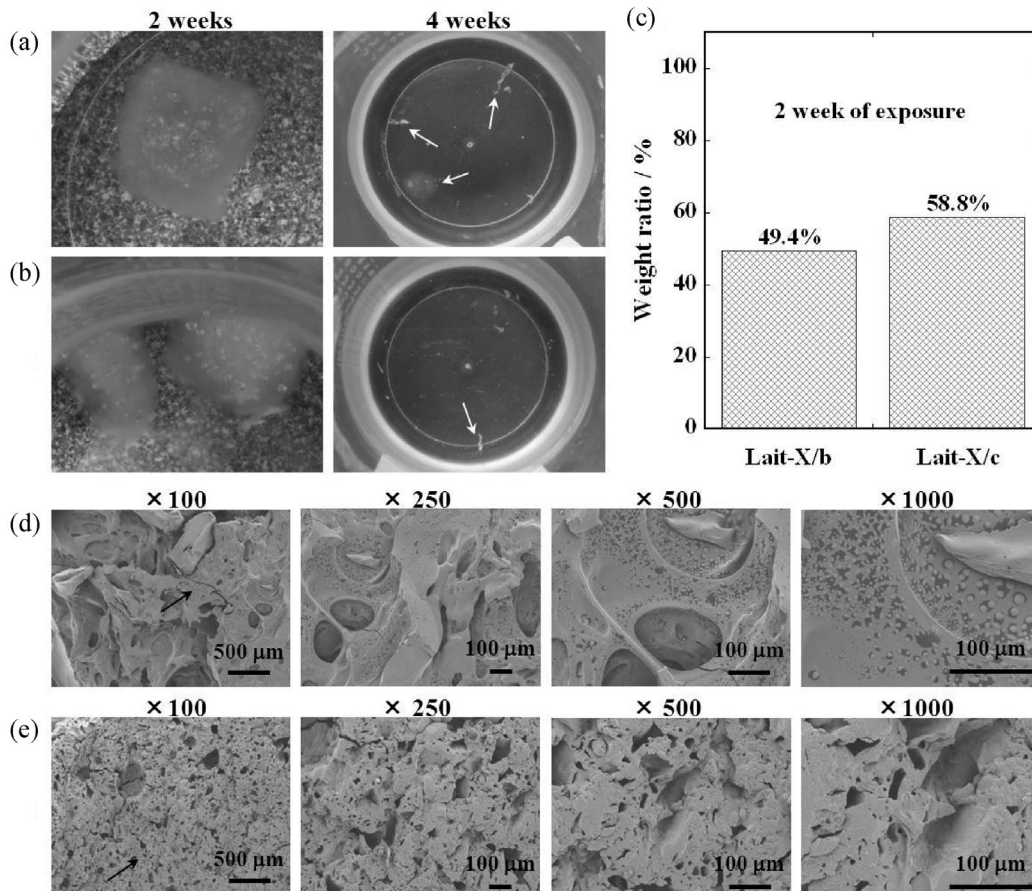


Figure 5. In vitro biodegradation analysis of scaffolds after two weeks of immersion in the PBS medium: (a) and (b) show the optical image of Lait-X/b and Lait-X/c, (c) the weight after in vitro degradation (%) of Lait-X/b and Lait-X/c, (d) and (e) shows FE-SEM of Lait-X/b and Lait-X/c for 100 \times , 250 \times , 500 \times , and 1 000 \times magnifications.

adhesion confirming the biocompatibility through the cell/scaffold interaction. The in vitro degradation of the PLA thermoset scaffolds was faster for the ones prepared by foaming and subsequent leaching. The results suggests that novel crosslinked PLA thermoset macroporous scaffolds with a porosity of 50% discussed in this study are stable and best suited for the bone tissue engineering applications.

Acknowledgements: This work was supported by KAKENHI (22656148) and the Strategic Research Infrastructure Project of the Ministry of Education, Sports, Science and Technology, Japan (2010–2014).

Received: December 14, 2011; Revised: January 25, 2012; Published online: May 7, 2012; DOI: 10.1002/mame.201100436

Keywords: bone tissue engineering; crosslinked polylactide; degradation; hMSC adhesion

- [1] K. F. Leong, C. K. Chua, N. Sudarmadji, W. Y. Yeong, *J. Mech. Behav. Biomed. Mater.* **2008**, *1*, 140.
- [2] S. Yang, K. Leong, Z. Du, C. Chua, *Tissue Eng.* **2001**, *7*, 679.
- [3] A. Salerno, S. Iannace, P. A. Netti, *Macromol. Biosci.* **2008**, *8*, 655.
- [4] D. W. Huttmacher, *Biomaterials* **2000**, *21*, 2529.
- [5] N. Virgilio, P. Sarazin, B. D. Favis, *Biomaterials* **2010**, *31*, 5719.
- [6] Y. Fujimoto, S. S. Ray, M. Okamoto, A. Ogami, K. Ueda, *Macromol. Rapid Commun.* **2003**, *24*, 457.
- [7] S. S. Ray, K. Yamada, M. Okamoto, K. Ueda, *J. Nanosci. Nanotechnol.* **2003**, *3*, 503.
- [8] Y. Ema, M. Ikeya, M. Okamoto, *Polymer* **2006**, *47*, 5350.
- [9] M. Bitou, M. Okamoto, *Polym. Degrad. Stab.* **2008**, *93*, 1081.
- [10] E. W. Washburn, *Phys. Rev.* **1921**, *17*, 273.
- [11] A. O. Helminen, H. Korhonen, V. Seppälä, *J. Polym. Sci., Part A: Polym. Chem.* **2003**, *41*, 3788.
- [12] A. O. Helminen, H. Korhonen, V. Seppälä, *J. Appl. Polym. Sci.* **2002**, *86*, 3616.
- [13] A. O. Helminen, H. Korhonen, V. Seppälä, *Polymer* **2001**, *42*, 3345.
- [14] K. Whang, K. E. Healy, D. R. Elenz, E. K. Nam, D. C. Tsai, C. H. Thomas, G. W. Nuber, F. H. Glorieux, R. Travers, S. M. Sprague, *Tissue Eng.* **1999**, *5*, 35.

- [15] J. J. Klawitter, S. F. Hulbert, *J. Biomed. Mater. Res. Symp.* **1971**, 2, 161.
- [16] V. Cannillo, F. Chiellini, P. Fabbri, A. Sola, *Compos. Struct.* **2010**, 92, 1823.
- [17] R. Langer, J. P. Vacanti, *Science* **1993**, 260, 920.
- [18] W. L. Grayson, M. Fröhlich, K. Yeager, S. Bhumiratana, M. Ete Chan, C. Cannizzaro, L. Q. Wan, X. S. Liu, X. E. Guo, G. Vunjak-Novakovic, *PNAS* **2010**, 107, 3299.
- [19] T. Dvir, B. P. Timko, M. D. Brigham, S. R. Naik, S. S. Karajanagi, O. Levy, H. Jin, K. K. Parker, R. Langer, D. S. Kohane, *Nat. Nanotechnol.* **2011**, 6, 720.
- [20] S. Wu, X. Liu, T. Hu, P. K. Chu, J. P. Y. Ho, Y. L. Chan, K. W. K. Yeung, C. L. Chu, T. F. Hung, K. F. Huo, C. Y. Chung, W. W. Lu, K. M. C. Cheung, K. D. K. Luk, *Nano Lett.* **2008**, 8, 3803.
- [21] M. N. Rahaman, D. E. Day, B. S. Bal, Q. Fu, S. B. Jung, L. F. Bonewald, A. P. Tomsia, *Acta Biomater.* **2011**, 7, 2355.
- [22] A. G. Gristina, M. Oga, L. X. Webb, C. D. Hobgood, *Science* **1985**, 228, 990.
- [23] J. Heisel, *Unfallchirurgie* **1987**, 13, 179.
- [24] R. A. White, J. N. Weber, E. W. White, *Science* **1972**, 176, 922.